International Journal of Applied Engineering Research ISSN 0973-4562 Volume 13, Number 20 (2018) pp. 14733-14740

A Novel Method for Denoising Remotely Sensed Hyperspectral Image Using Autoencoder Technique

Shivakumar B R[1], Dr. Prakash J[2]

[1]*Research Scholar, VTU, Belagavi, Department of Information Science and Engineering, Bangalore Institute of Technology, K. R. Road, V.V. Puram, Bengaluru, India.*

[2] *Professor and Head, Department of Information Science and Engineering, Bangalore Institute of Technology, K. R. Road, V.V. Puram, Bengaluru, India.*

Abstract

Denoising of Hyper-spectral imagery (HSI) is an essential stage prior to further processing such as dimensionality reduction, classification and object identification. The traditional noise reduction filtering techniques may not preserve the information across the spectral bands. Hence the information loss leads to performance degradation in advanced processing stages. This paper proposes denoising of HSI using stacked autoencoders, in which concept of deep neural network is used. Particularly, this model is experimented to determine the degree of reconstruction of HSI image in which, it improves the perception quality of the inherent noisy bands and also reconstructs the normal bands with negligible changes. The proposed method has been used to experiment the robustness of the model against input images with various quantity of noise. The comprehensive evaluation of the model is extended by computing the statistical parameters Peak signal to Noise Ratio (PSNR), Image quality Index (IQI), Mutual Information (MI) and entropy. The performance of the model is analysed by signal analysis, visual inspection of different bands, comparison of spectral signature of pixels. The proposed algorithm demonstrated that stacked autoencoder is better solution for noise reduction in Hyperspectral images with different noise densities.

Keywords: Autoencoder, deep neural networks, Denoising, Hyper-spectral image, spectral signature analysis, stacked autoencoder.

INTRODUCTION

The ever increasing demand of increased resolutions in spectral, temporal and radiometric parameters of observations in remote sensing, leads to multispectral and Hyperspectral imagers. HSI measures reflected radiance as a series of narrow and contiguous wavelength bands with finer resolution. Though most HSI measure hundreds of spectral bands, it is not the number of measured bands that qualifies a sensor as Hyperspectral rather narrowness and contiguous nature of measurements. Some HSI sensors such as Airborne Visible/Infrared Imaging Spectrometer(AVIRIS) spans the bandwidth between 400nm to 2500nm with 224 bands as shown in Fig 1(a).

For a given Hyperspectral pixel vector $\mathbf{P} = (p_1,p_2,\ldots p_L)^T$, each component p_i represents a pixel in band image $\mathbf{B_l}$ which is captured by a certain wavelength $\mathbf{W_l}$ in a specific spectral range. Let $\mathbf{S}=(S_1,S_2,\ldots,S_L)^T$ be the corresponding spectral signature of P as shown in Fig 1(b). Here S_l represents the spectral signature of p_l in the form of radiance or reflectance value. For example, typically L can be of 224 bands and the spectral range **W** may be between 400nm to 2500nm, which covers visible spectrum and infrared region of the spectrum.

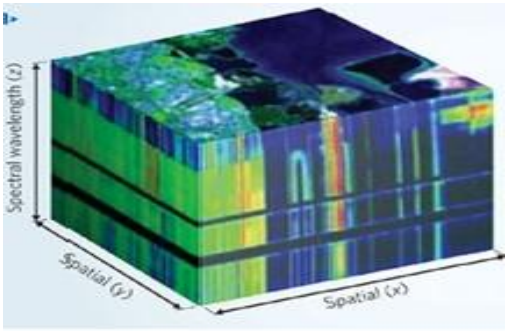

1(a). 3-D representation of Hyperspectral image where x and y-axis represents the spatial information and z-axis represents the spectral information.

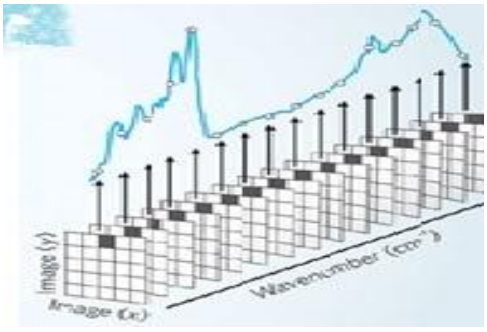

1(b). The spectral signature of a pixel

Figure 1. HSI cube representation.

HSI provides information through huge number of spectral channels. A typical application may need certain spectral bands of objects being observed. The spectral reflectance and absorption characteristics of matters or objects are to be known prior to analyzing the Hyperspectral data. The content, concentration, structure and constituents of the matter influence the spectral signature[5],[17]. The rate of degradation and depletion of resource has accelerated tremendously in view of ever increasing demographic pressure. Deforestation, desertification, soil erosion and salinisation have degraded the environment, threatening the food security and economic development of many countries. The HSI can be used to monitoring and management of the resources such as in the application of precision farming, mineral mapping and water (Inland, coastal and open ocean), military monitoring[10]. The acquired HSI may affected from noise contamination, stripe corruption, calibration error, photon effect or mixture of various noises such as Gaussian, impulse noise or dead pixels or combinations of two or more specified[1].The quality of HSI degraded by various types of noise which in turn reduces the performance of the HSI processing tasks such as classification, spectral unmixing, segmentation and matching.

The organisation of the paper is as follows. The related works of identifying technology, methodology, results and application in section II, Section III explains the architecture and methodology of the proposed algorithm, section IV describes the experimental results and section V presents evaluation of the model for the implicit and explicit noise factors. The concluding remarks is presented in section VI.

LITERATURE SURVEY

In recent years, varieties of noise reduction techniques for HSI are introduced by applying them on various datasets and conditions. Traditionally, [18] each band of HSI which is represented by 2-D matrix or vector considered for the application of filters, which convolves with sliding window in the image domain. The Discrete Wavelet Transformation(DWT)[11] is also applied to reduce the noise of the individual bands by suppressing the high frequency components. The individual band noise reduction techniques decorrelates the spatial bands and hence the loss of information across the spectral bands. To address this phenomena, a combination of spatial and spectral wavelet shrinkage technique[19] has been proposed which works in spectral derivative domain. In case of multispectral and Hyperspectral Images, the dimensionality of the images are high. Therefore, using the correlation between the adjacent bands[12], the denoising techniques can be applied. In this method, the data is projected on to the subspace, while noise and some high frequency components are eliminated and useful information is preserved. The Minimum Noise Fraction(MNF) transformation is used to reduce the dimensionality of HSI by segregating the noise in the data. The MNF is a linear transformation and it is a two cascaded Principal Component Analysis(PCA). The first transformation estimates noise covariance matrix and rescales the noise in the data. The second transformation is a standard PCA of the noise whitened data. The MNF transformation[14] computes the normalized linear combinations of the original bands which maximizes the signal to noise ratio. The number of noisy component estimation is different for individual band with different Signal Noise Ratio(SNR), hence it is difficult to achieve the optimal denoising simultaneously for all the bands.

In the case of unmixing based denoising, as a first step, a set of reference spectra is produced by averaging the neighboring pixels in each class of interest. After, [16]each pixel which is linear combination of the reference spectrum and residual vector, which quantifies the unmixing error is computed. Therefore, individual pixel spectrum can be reconstructed without residual error, which leads to denoising of HSI. The whole HSI image is considered as third order tensor and it is subdivided in to sub-blocks, subsequently, similar blocks are clustered and stacked to construct fourth order tensor. The noise is reduced by determining the lower dimensional approximation by Tucker Factorization[7]. The mixture of Gaussian noise and sparse noise are reduced using low rank tensor recovery technique. This technique preserves the global structure of Hyperspectral image and reduces the Gaussian and sparse noise effectively[1]. In deep neural network, unsupervised learning of a representation in which the learned models are robust to partial corruption of the input pattern. This approach is used to train auto encoders, such that , the learnt auto encoders produce same representation, albeit partially destroyed inputs are fed to it[15]. In case of unmixing operation on noisy HSI, part-based denoising auto encoder is used to minimize the reconstruction error and redundant end members simultaneously[2]. The denoising auto encoders detects edge in natural image and larger strokes in digit images. It shows that it is possible to prove denoising criterion as a the learning of useful higher level representations by unsupervised training. The reconstruction of input is merely not sufficient to assure the extraction of features, which maximizes the mutual information, but it is essential to obtain the clean input robustly from the corrupted or noisy input[13].

PROPOSED METHODOLOGY

This section presents the architecture, working principle and the algorithm of the proposed methodology for denoising HSI using autoencoder technique. The architectural diagram of the proposed method is presented as shown in Fig 2, which takes the pixel vector P as an input to the network and train the autoencoder model in unsupervised manner to reconstruct the input pixel P, at the output O. To improve the robustness of the autoencoder model, the input pixel P is partially added with noise, which is denoted as $\tilde{P}$ is fed to the model while training. The autoencoder model is trained such a way that denoised P will be reconstructed by mapping $\tilde{P}$ to the P.

The autoencoder model uses multilayer Back Propagation Artificial Neural Network to denoise the Hyperspectral images[8]. This model has one visible input layer of L nodes, three hidden layers of different number of nodes and one visible output layer of L nodes.

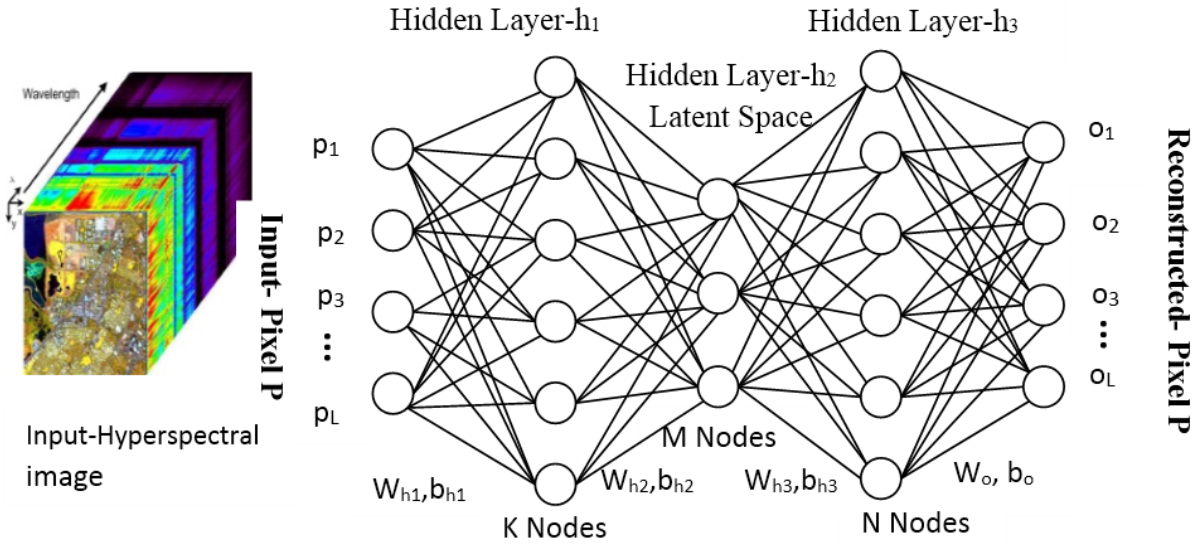

Figure 2. A Multi layer denoising autoencoder for HSI.

During data processing, the input pixel P of L bands maps to the hidden layer h_1 by the dimension $p \in R^L$ and get to hidden layer h_1 representation $h_1 \in R^K$, and then h_1 maps to latent space representation $h_2 \in R^M$. Similarly, latent space h_2 maps to h_3 by $h_3 \in R^N$. Finally the hidden layer h_3 ends at output layer as same size as the dimension of P that is $o \in R^L$, which is called as reconstruction layer as presented in Fig 2. The computational procedure is expressed mathematically by referring the notation which are used in Fig 2.

$$h_{1net} = f(W_{h1}, b_{h1}) \quad \text{.....(1)}$$

where $h_{1net} = b_{h1} + \sum_{j=1}^{L} WjPj$ for all K nodes and b_{h1} is the bias at h_1 layer.

The activation function[3], Rectified Linear Unit (ReLU) is used to threshold the activation at zero, which accelerates the convergence of the stochastic gradient descent. The mathematical expression for ReLU is given as eq (2) which is applied to all the nodes of hidden layers h_1,h_2 and h_3.

$$h_{1i} = f(h_{1net}) = max(0, h_{1net}) \quad \text{.....(2)}$$

Similarly for successive layers, it is shown that

$$h_2 = f(W_{h2}, b_{h2}) \quad \text{.....(3)}$$

$$h_3 = f(W_{h3}, b_{h2}) \quad \text{.....(4)}$$

$$o = f(W_o, b_o) \quad \text{.....(5)}$$

In the reconstruction layer, the activation function used is Sigmoidal function which is given in eq (6) , which softens the activation which is applied to all the nodes from $o_{1\,net}$ to $o_{L\,net}$.

$$o_i = f(Oi\,net) = \frac{1}{1+e^{-oi\,net}} \quad \text{.....(6)}$$

where $O_{inet} = b_{o1} + \sum_{j=1}^{N} W_j h_{3j}$ for all L nodes and b_{o1} is the bias at output layer

The main intention of training the model is to minimize the reconstruction error between input p and output pixel o, where C is a Cost function or Loss function, which is given as in eq (7). The mean square error is used as loss function which is expressed in eq (8).

$$p, o = argmin[C(p^{(i)}, o^{(i)})] \quad \text{.....(7)}$$

$$C(w,b) = \frac{1}{2n}\sum_p \|p - o\|^2 \quad \text{.....(8)}$$

where w is the set of all weights, b is the biases, n is the number of training samples , p is the set of input and o is the actual output for the input p.

The cost function is differentiated to obtain the sensitivity of the error for each output layer node. The product of learning rate (value varies from 0 to 1) and the rate of change of cost is back propagated to the network till the input end by modifying the link weights, therefore the error will be minimized by converging the weights of the network to the optimal values.

A. Algorithm for Denoising Autoencoder Training and Testing

The steps involved in the training and testing of denoising autoencoder are listed as below.

Step 1: Building of the Network

i. Create feed-forward multi layer network with L inputs, hidden layer h_1,h_2,h_3 and o with K,M,N and

L number of nodes respectively as shown in Figure 2.

ii. The ReLU activation function as in eq. (2) is set to all the nodes of hidden layers and Sigmoidal activation function as in eq. (6) is set to output layer o.

Step 2: Preparation of the Dataset

(i) Normalize all the pixel value of the image that is scale down the pixel value [0-255] to [0.0-1.0]

(ii) Choose any particular band add Gaussian Noise in certain percentage from 0% to 100%.

(iii) Read the Hyperspectral image of the size Row R x Column C x Bands L, pixel by pixel as a training sample.

(iv) Shuffle the samples.

(v) Split the RxC number of pixels in the ratio of 6:2:2, in which 60% of pixels will be used for training,20% for validation and remaining 20% for testing purpose.

Step 3: Initialization of the Model

(i) Initialize all network weights and biases to random numbers.

(ii) Initialize the learning rate to 10^{-3}.

(iii) set the Loss function as given in eq.(8) and the optimizer.

Step 4:Training

i. Until the termination condition is met, Do

ii. For each epoch, Do

iii. Input the pixel p to the network and compute the o_i of every unit i in the network.

iv. For each network unit node, compute net value as in equation (1) and compute output of each node after applying activation function as given in equation (2).

v. For each hidden node h_{ij}, compute the error as in equation (8).

vi. Update each network weight by w = w+Δw, where Δw=αδp, α → learning rate, δ → rate of change of error,

i. p→ input to that node

vii. Back propagate the error until it reaches the first layer and update the weights.

viii. Go to Step 4(ii)

ii. xi. Stop when training samples exhausted or termination condition is met.

Step 5: Testing

i. Consider testing sample pixels and feed them to the network as described in step 4. The weights of the network should not be updated.

ii. The actual output is compared with the input pixel vector. The error is computed.

iii. If the accuracy is up to the desired one go to Step 7.

Step 6: Fine tuning of the model

a. If the accuracy is not up to the expected value, modify the hyper parameters such as learning rate, cost function, number of hidden layers, no. of nodes in hidden layers, regularizer function. Go to Step 1 and repeat the training.

Step 7: The model is ready with the optimized weights, can be used for application.

Then, the noisy images can be fed to the model and obtained denoised images.

EXPERIMENTAL RESULTS

This section presents the experimental results of the proposed methodology. In this experiment, the denoising stacked auto encoder network has been built with one input layer with 220 nodes, 4 hidden layers with 300, 200, 100, 200 nodes and output layer with 220 nodes. About 21000 sample pixels are shuffled and consequently divided as training data, validation data and testing data with a ratio 6:2:2. The training data are used for updating of weights and testing data is used for algorithm evaluation. In the experiment, mean squared error loss function is used for computing the error and to penalize the large magnitude weights in the network L1 regularizer is applied with the factor of 0.1. The learning rate has been tuned in the range between 10^{-2} to 10^{-6}.

For experimentation, AVIRIS Hyperspectral image of Indianpines[4] is applied to assess the proposed denoising of HSI by auto encoder technique. This image has been collected over 2 miles by 2 miles area (contains 145x145 pixels) of the Indianpines test site in north-west Indiana, USA. It has spatial resolution of 20m with 224 spectral bands in the wavelength range 400nm to 2500nm. The image scene is containing $2/3^{rd}$ of agricultural land and $1/3^{rd}$ of forest vegetation. There are highways, railway lanes and also few housing structures present in the image. There are 16 classes of data samples namely woods, stone-steel tower structures, fields of corn, soybean, wheat and other objects.

The experiment is carried out with the proposed method to determine, mainly two factors, (i) To verify the degree of reconstruction of the clean input image and (ii)To measure the robustness of the algorithm to the noisy input image. The Indianpines dataset has the water absorption bands of 104 to 108,150 to 163 and 220 and these bands are intrinsically noisy in visual appearance as shown in Fig 4(a) through 4(c) . To test the first hypothesis, the original data set was used to train the model in unsupervised mode for reconstruction of the input image. The metrics such as Peak Signal to Noise Ratio (PSNR) [9], the image Quality Index, Mutual Information, Entropy of Images are determined for both water absorption bands and normal bands. The result is given in Table I, for the bands 104, 150, 220 (water absorption bands) and 10, 73, 200 (Normal Good Bands). From the Table I, it is observed that, the reconstructed water absorption bands are not similar to the original input bands. From these bands, it is observed that more features can be extracted compared to original bands and have better visualization as shown in Fig 4(d) through 4(f). The metrics for normal good bands 10, 73 and 200 shows

significant performance improvement after reconstruction and as shown in Fig. 3(a) through 3(f). It is identified by the visual inspection and through various parameters computed as in Table II, features are significantly retained after reconstruction with minimal changes.

The proposed method is tested by the following metrics to measure the quality of the reconstructed image, which are given in equation (9) and (10)

$$\text{PSNR} = 20\log\frac{255}{\sqrt{MSE}} \quad \text{.....(9)}$$

where

$$\text{MSE} = \frac{1}{RC}\sum_{Y=1}^{R}\sum_{X=1}^{C}\left[I_{ip}(X,Y) - I_{rcon}(X,Y)\right]^2 \text{.....(10)}$$

where R-Number of Rows; C- Number of Columns, I_{ip}-Input image band, I_{rcon}-Reconstructed Image band.

Image Quality Index(IQI) is combination of loss of correlation, luminance distortion, and contrast distortion, which is used to measure the distortion between reference and noisy image[20]. The mutual information between input and output image is determined to find the degree of statistical dependency[16].

Table I. Reconstruction without external noise addition

Metric	Water absorption Noisy Bands			Normal Good Bands		
	B104	B150	B220	B10	B73	B200
PSNR	31.45	25.29	30.57	53.37	56.76	41.53
Image Quality Index	0.06	0.07	0.07	0.86	0.92	0.58
Mutual Information	0.294	0.20	0.179	2.44	2.76	1.74
Entropy Output Image	6.69	6.19	6.41	7.03	6.96	7.21

Table II. Reconstruction of HSI with Gaussian noise from 10% to 50%

Metric	**Noise Factor**				
	0.1	0.2	0.3	0.4	0.5
PSNR	48.64	42.29	33.16	20.39	19.1
Image Quality Index	0.77	0.44	0.18	0.03	0.03
Mutual Information	2.18	1.43	1.02	1.07	0.99
Entropy of Output Image	7.11	7.29	7.50	7.82	7.66

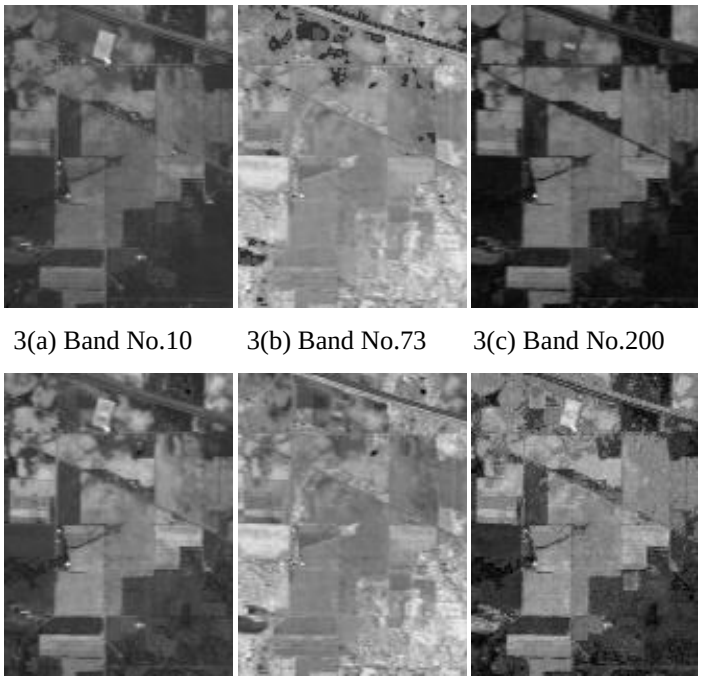

3(a) Band No.10 3(b) Band No.73 3(c) Band No.200

3(d) Band No.10 3(e) Band No.73 3(f) Band No.200

Figure 3. Reconstruction of normal bands (a) through (c) Original Image. (d) through (e) Reconstructed Image

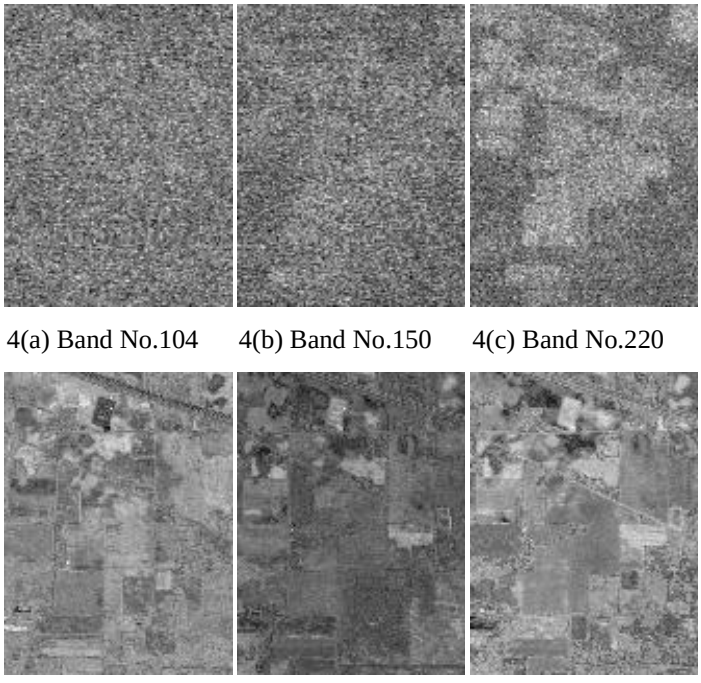

4(a) Band No.104 4(b) Band No.150 4(c) Band No.220

4(d) Band No.104 4(e) Band No.150 4(f) Band No.220

Figure 4. Reconstruction of Water absorption Noisy bands (a) through (c) Original Image. (d) through (e) Reconstructed Image

To measure the robustness of the model to the noisy input image, the 10th band of input image is added with different quantity of Gaussian noise from σ = 0.1 to 0.5. The image

with the noisy band is used to train the autoencoder model by considering original image as a target. After the training of the model, the input image with noisy band as shown Fig. 5(a) through 5(c) is fed to the model. The reconstructed, denoised image is shown as in Figure 5(d) through 5(f). Then the reconstructed output image compared with the original image using the metric as shown in Table II. The training helps in generalization of the model, therefore the weights in the network updated which ensures the denoising of the noisy input images. The result shows that the model reconstructs and denoise the input noisy image robustly, with better retention of the features of HSI.

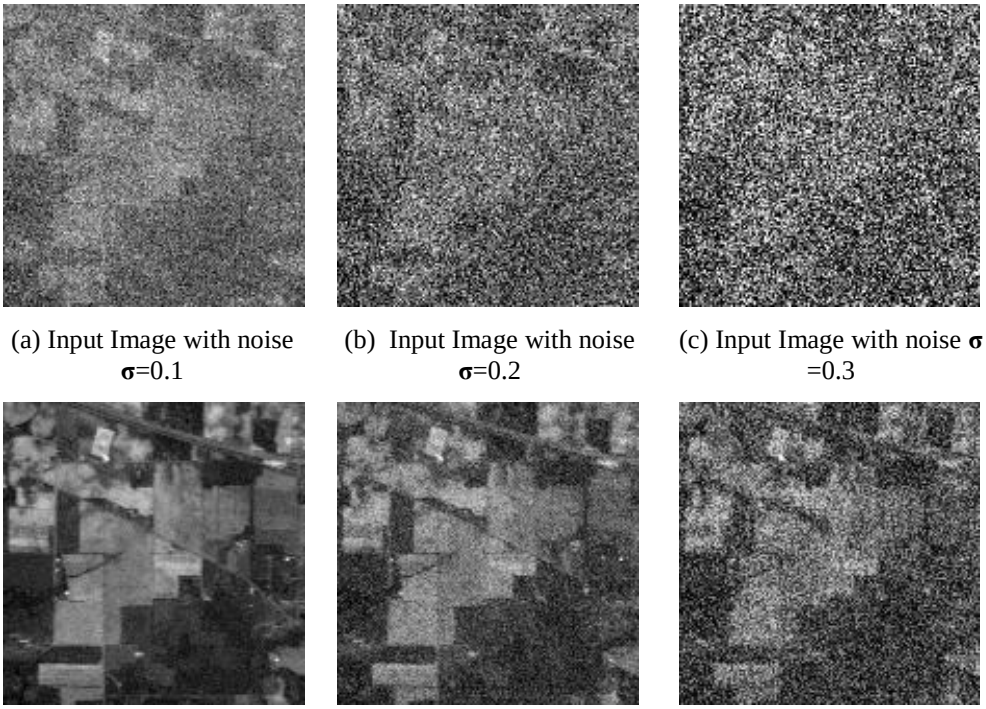

(a) Input Image with noise **σ**=0.1 (b) Input Image with noise **σ**=0.2 (c) Input Image with noise **σ** =0.3

(d) Output image for **σ**=0.1 (e) Output image for **σ**=0.2 (f) Output image for **σ**=0.3

Figure 5. Reconstruction of band 10 which is added with Gaussian Noise

PERFORMANCE ANALYSIS

The performance of the proposed methodology is evaluated by using spectral signature analysis and signal analysis.

A. Spatial Signal analysis

The noise in the image randomly vary to the extreme values compared to natural image pixels. Therefore, to evaluate the impact of noise in spatial context, the signal analysis has been carried out. Typically, Band 10 is added with Gaussian noise of $\sigma = 0.1$ and fed to the model. The reconstructed output image signal is plotted along with noisy signal as shown in Fig. 6. The reconstructed signal is close to the original image signal rather than noisy signal. Hence, the model is robust for the external noise influence.

B. Spectral Signature analysis

The pixel of a scene may contain various types of objects, vegetation and land cover. The spectral reflectance and absorption characteristics of the objects of the scene are called as spectral signature. It is desirable that, the denoising process should not distort the signature of a pixel. To examine the effect of the proposed methodology in signature distortion, the spectral signature of a pixel is studied. The spectral signature of original image pixel is compared with the reconstructed image pixel feature as shown in Fig. 7(a). It is observed that the output pixel follows spectral signature of the input pixel with minimal distortion. Similarly the reconstructed signature obtained by feeding the noisy image with the noise quantity $\sigma = 0.1$ to 0.5 is shown in Figure 7(b) through 7(d). By this analysis, it is evident that the model is more robust to the noise and the impact of noise at one band is not affected on its neighbourhood bands.

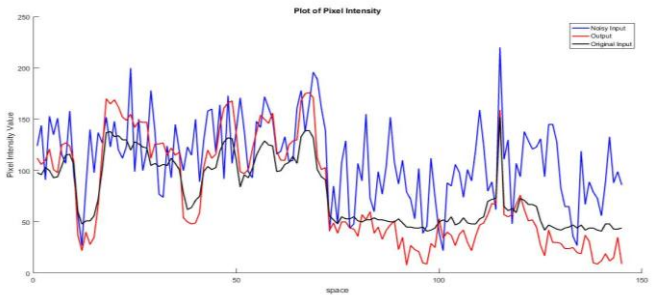

Figure 6. Signal Analysis for Band 10 at Gaussian Noise factor $\sigma = 0.1$

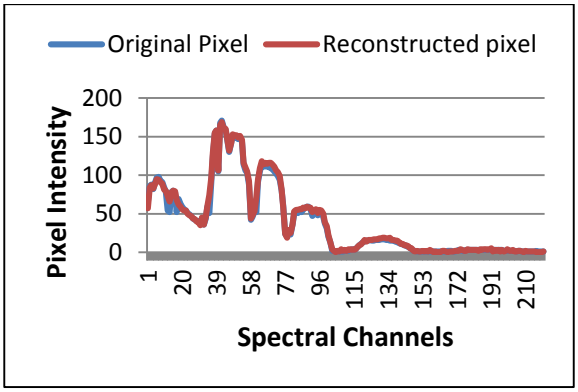

(a) Reconstruction of input pixel without Noise

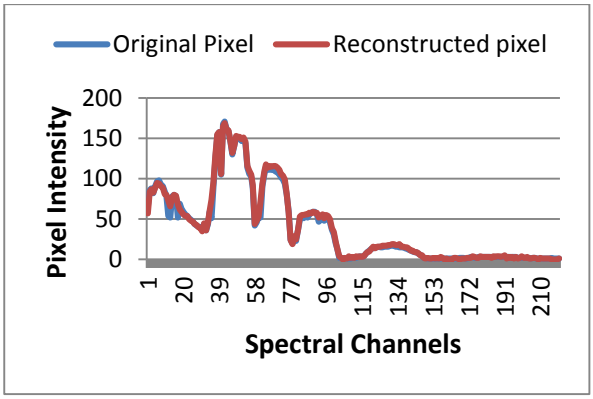

(b) Reconstruction of Noisy pixel σ = 0.1

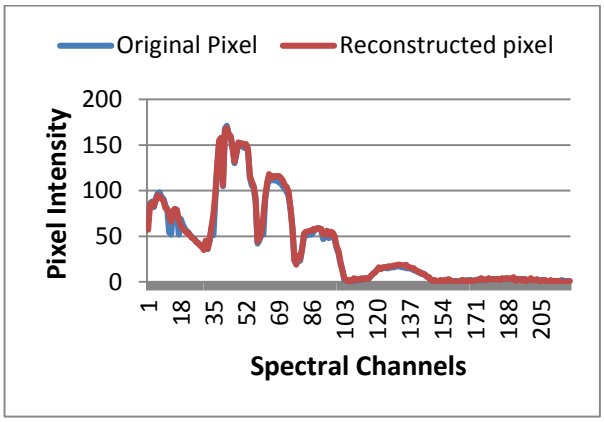

(c) Reconstruction of Noisy pixel σ = 0. 3

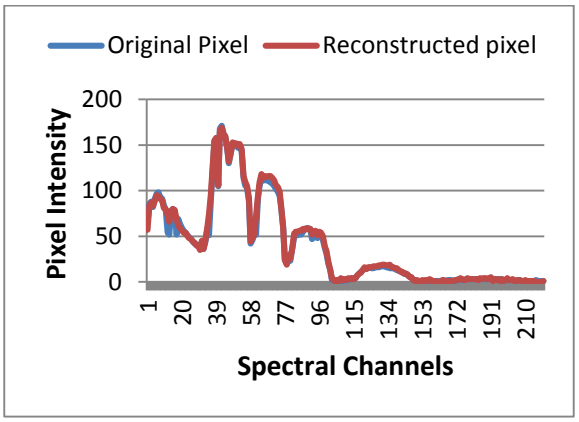

(d) Reconstruction of Noisy pixel σ = 0.5

Figure 7. (a) Reconstruction of input pixel without adding noise 6(b) through (d). Reconstruction of input pixel after introducing Gaussian noise of different quantity to Band 10.

CONCLUSION

A novel method proposed for reconstruction and denoising of Hyperspectral image using stacked autoencoder which uses deep neural network is presented. The experimental result shows that, the proposed method improves the perception quality of the reconstructed, noisy water absorption bands. It is also shown that, normal bands are reconstructed with high PSNR, Image Quality Index and mutual information. The experiment also proved that, the proposed model is more robust to the noisy input. Hence without using any conventional filters in the model, the noise in the image is reduced without affecting the neighbour bands. Therefore the information across spectral bands is preserved. The future work involves, the proposed model will be more generalized and used as pre-processing module for dimensionality reduction, classification of wide range of Hyperspectral images.

ACKNOWLEDGEMENT

The authors are grateful to the Research and Development centre, Information science and Engineering, Bangalore Institute of Technology for providing us facilities to carry out our research work. The authors also thank management of BIT, Visvesvaraya Technological University (VTU), Belgaum for their timely kind cooperation.

REFERENCES

[1] Haiyan Fan, Yunjin Chen,Yulan Guo, Hongyan Zhang, "Hyperspectral Image Restoration Using Low-Rank Tensor Recovery", in *IEEE Journal of Applied Earth Observations and Remote Sensing*,Vol. 10, No.10,October 2017.

[2] Ying Qu, Rui Guo, and Hairong Qi,"Spectral Unmixing Through Part-Based Non-Negative Constraint Denoising Autoencoder", in *IGARSS 2017*.

[3] Chen Xing,1 Li Ma, and Xiaoquan Yang," Stacked Denoise Autoencoder Based Feature Extraction and Classification for Hyperspectral Images", in *Journal of Sensors*, Volume 2016, Article ID 3632943.

[4] Baumgardner, M. F., Biehl, L. L., Landgrebe, D. A. (2015). 220 Band AVIRIS Hyperspectral Image Data

Set:June12,1992 Indian Pine Test Site 3. *Purdue University Research Repository*.

[5] Charles E. Glass," Interpreting Aerial Photographs to Identify Natural Hazards ", in *sciencedirect, Earth and planetaryscience*, 2013

[6] Daniele Cerra, Rupert M¨uller, and Peter Reinartz,"Noise Reduction in Hyperspectral Images Through Spectral Unmixing", *IEEE Geoscience And Remote Sensing*, 2013

[7] Danping Liao, Minchao Ye, Sen Jia and Yuntao Qian, "Noise Reduction of Hyperspectral Imagery based on Non Local Tensor Factorization", *IGARSS,2013*

[8] Zhouhan Lin, Yushi Chen, Xing Zhao, Gang Wang," *Spectral-Spatial Classification of Hyperspectral Image Using Autoencoders*",in *ICICS 2013*.

[9] Yuheng Chen, Yiqun Ji etal "Computation of Signal-to-noise Ratio of Airborne Hyperspectral Imaging Spectrometer", in *International Conference on Systems and Informatics (ICSAI 2012)*

[10] Azam Karami,Mehran Yazdi, and Zolghadre Asli, "Noise Reduction of Hyperspectral Images using Kernel Non-Negative Tucker Decomposition", in *IEEE Journal of Signal Processing*,Vol. 5,No.3,June 2011

[11] Faten Ben Arfia, Abdelouahed Sabri, Mohamed Ben Messaoud, Mohamed Abid," The Bidimensional Empirical Mode Decomposition With 2d-Dwt For Gaussian Image Denoising", in *17th International Conference on Digital Signal Processing (DSP)*, Year: 2011,Pages: 1 - 5

[12] G.Chen and S.E. Qian, "Denoising of hyperspectral imagery using principal component analysis and wavelet shrinkage", in *IEEE Trans.Geosci. Remote Sens.*, vol. 49, no. 3, pp. 973–980, Mar. 2011.

[13] Pascal Vincent, Hugo Larochelle etal," Stacked Denoising Autoencoders: Learning Useful Representations in a Deep Network with a Local Denoising Criterion", in *Journal of Machine Learning Research*,11, 3371-3408, 2010.

[14] U. Amato, R. M. Cavalli, A. Palombo, S. Pignatti, and F. Santini,"Experimental approach to the selection of the components in the minimum noise fraction", in *IEEE Trans. Geosci. Remote Sens.*, vol. 47,no. 1, pp. 153–160, Jan. 2009

[15] Pascal Vincent, Hugo Larochelle, Yoshua Bengio, Pierre-Antoine Manzagol," Extracting and Composing Robust Features with Denoising Autoencoders", in *Proceedings of the 25th International Conference on Machine Learning*, Helsinki, Finland, 2008.

[16] M. Ceccarelli, M. di Bisceglie, C. Galdi, G. Giangregorio, S.L. Ullo, "Image Registration Using Non–Linear Diffusion", in *IGARSS 2008.*

[17] Marcus Borengsser,Williams S.Hungate,Russell Watkins,"Hyperspectral Remote sensing principles and applications*", CRC Press*,USA,2008.

[18] R.C.Gonzalez and R.E.Woods,*Digital Image Processing*, 3rd Edition, Prentice-Hall, *USA,*Aug. 2007.

[19] H. Othman and S. Qian, "Noise reduction of hyperspectral imagery using hybrid spatial-spectral derivative-domain wavelet shrinkage," in *IEEE Trans. Geosci. Remote Sens.*, vol. 44, no. 2, pp. 397–408, Feb.2006.

[20] Zhou Wang, Alan C. Bovik, "A Universal Image Quality Index", in *IEEE Signal Processing Letters,* Vol. 9, No. 3, March 2002.